



**HAL**  
open science

# Control of the mobilization of arsenic and other natural pollutants in groundwater by calcium carbonate concretions in the Pampean Aquifer, southeast of the Buenos Aires province, Argentina

M. Vital, D.E. Martínez, P. Babay, S. Quiroga, A. Clement, Damien Daval

## ► To cite this version:

M. Vital, D.E. Martínez, P. Babay, S. Quiroga, A. Clement, et al.. Control of the mobilization of arsenic and other natural pollutants in groundwater by calcium carbonate concretions in the Pampean Aquifer, southeast of the Buenos Aires province, Argentina. *Science of the Total Environment*, 2019, 674, pp.532-543. 10.1016/j.scitotenv.2019.04.151 . hal-02372351

**HAL Id: hal-02372351**

**<https://hal.science/hal-02372351v1>**

Submitted on 20 Nov 2019

**HAL** is a multi-disciplinary open access archive for the deposit and dissemination of scientific research documents, whether they are published or not. The documents may come from teaching and research institutions in France or abroad, or from public or private research centers.

L'archive ouverte pluridisciplinaire **HAL**, est destinée au dépôt et à la diffusion de documents scientifiques de niveau recherche, publiés ou non, émanant des établissements d'enseignement et de recherche français ou étrangers, des laboratoires publics ou privés.

1                   **Control of the mobilization of arsenic and other natural pollutants in groundwater by calcium**  
2  
3                   **carbonate concretions in the Pampean Aquifer, southeast of the Buenos Aires province,**  
4  
5                   **Argentina.**  
6

7  
8  
9                   M. Vital<sup>1\*</sup>, D. E. Martinez<sup>1</sup>, P. Babay<sup>3</sup>, S. Quiroga<sup>4</sup>, A. Clement<sup>2</sup>, D. Daval<sup>2</sup>  
10

11  
12                   <sup>1</sup>Instituto de Geología de Costas y Cuaternario (UNMDP-CIC) – Instituto de Investigaciones Marinas y  
13                   Costeras (CONICET-UNMDP). Mar del Plata, Argentina.  
14

15  
16                   <sup>2</sup>Université de Strasbourg/EOST, CNRS, Laboratoire d'Hydrologie et de Géochimie de Strasbourg, 1  
17                   rue Blessig, F-67084 Strasbourg Cedex, France  
18

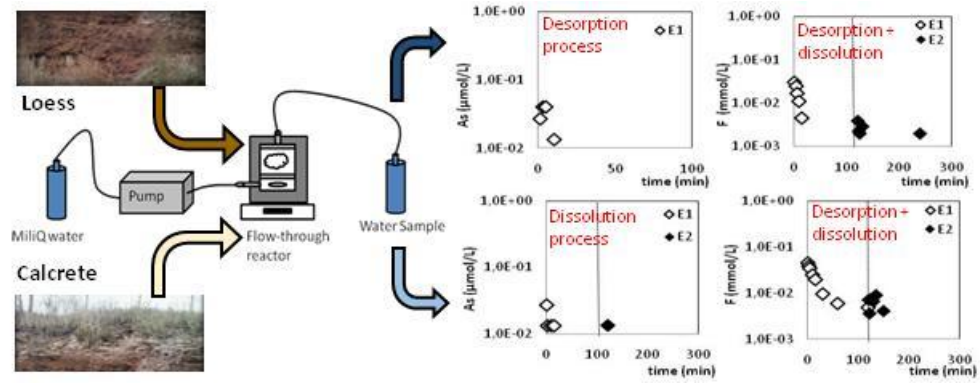
19                   <sup>3</sup>Comisión Nacional de Energía Atómica. Centro Atómico Constituyentes. Av. Gral. Paz 1499, B1650  
20                   Villa Maipú, Pcia de Buenos Aires  
21

22                   <sup>4</sup> Departamento de Química, Universidad Nacional de Mar del Plata, Argentina  
23

24  
25  
26  
27  
28                   \* corresponding autor : [ingagr.melanie.vital@gmail.com](mailto:ingagr.melanie.vital@gmail.com)  
29  
30  
31  
32  
33  
34  
35  
36  
37  
38  
39  
40  
41  
42  
43  
44  
45  
46

47                   *Submitted to Science of the Total Environment*  
48  
49  
50  
51  
52  
53  
54  
55  
56  
57  
58  
59  
60  
61  
62  
63  
64  
65

### GRAPHICAL ABSTRACT



## HIGHLIGHTS

- The origin of As, F and other pollutants in groundwater is still misunderstood.
- Consumption of water with high content of As is a major threat for human health.
- Time-resolved experiments were used to study elemental release in water.
- As, V, Ba, Sr are probably coprecipitated with calcite and F adsorbed on calcite.
- The mobility of pollutants in the Pampean Aquifer is controlled by calcrete.

1    **ABSTRACT**

2    The water supply for human consumption in the Chaco-Pampean region in Argentina is  
3    restricted by the low quality of groundwater due to elevated concentrations of arsenic and  
4    other trace elements. Previous studies indicated a complex concurrence of factors and  
5    processes that are believed responsible to control the distribution of arsenic in groundwater.  
6    For a better understanding of the origin of trace elements in the Pampean aquifer, flow-  
7    through experiments with loess and calcrete samples representative of the sediments that  
8    constitute the aquifer were carried out in continuous flow reactors. The aqueous solutions  
9    were collected and the concentrations of  $\text{SiO}_2(\text{aq})$ ,  $\text{Ca}^{2+}$ ,  $\text{SO}_4^{2-}$ ,  $\text{Na}^+$ ,  $\text{Cl}^-$ ,  $\text{F}^-$  and trace elements  
10   (Ba, Sr, V, and As) were measured by inductively coupled plasma atomic emission spectroscopy  
11   (ICP-AES), high performance liquid chromatography (HPLC) and capillary electrophoresis. The  
12   experiments showed differences in the release rate of elements to the solution according to  
13   the type of sediment. The highest concentrations of V, Ba, and As were measured in  
14   experiments conducted with loess, and these elements were released quickly to the solution in  
15   the first minute of the test. In the case of loess, V and As are suggested to be adsorbed on the  
16   solid particles surface. Conversely, the experiments conducted with calcrete showed a lower  
17   but continuous release of those elements. This last result may indicate that the trace elements  
18   were coprecipitated in the calcite. In addition, it was demonstrated that F did not come from  
19   the dissolution of minerals such as fluorapatite, but both desorption from solid surface and  
20   dissolution from calcite minerals account for the release of F. This study support that both  
21   dissolution and adsorption-desorption processes can control the mobility of trace elements,  
22   with an emphasis on the role of calcrete in the retention and the mobilization of trace  
23   elements in the Pampean aquifer.

24    **Keywords:** Arsenic - carbonate concretions - loess - groundwater contamination –kinetic  
25    modeling – Pampean aquifer

## 26 INTRODUCTION

27 Arsenic dissolved in water is one of the most important concerns regarding drinking  
28 uses in many areas of the world. Naturally-occurring high arsenic (As) groundwater  
29 concentrations are widely distributed in some large regions of different countries, including  
30 the USA (Scanlon et al., 2009; Chappells et al., 2014), Mexico (Wurl et al., 2014), Argentina  
31 (Nicolli et al., 1989; Gomez et al., 2009), China (Guo et al., 2015), Chile (Sancha and O’Ryan,  
32 2008), Vietnam (Erban et al., 2013), India (Chakraborti et al., 2016) and Bangladesh (Fendorf et  
33 al., 2010). The consumption of water with high concentration of As is related to arsenicosis,  
34 being an important threat for human health (Agusa et al., 2014; Joseph et al., 2015). About 140  
35 million people in the world are exposed to As contaminated drinking waters. Other trace  
36 elements such as fluoride and vanadium are also of concern for human health. High fluoride  
37 concentrations in waters are associated with dental fluorosis and sometimes bone fluorosis  
38 (Sota de la et al., 1997), while vanadium can cause aneugenic effects and irritation of the  
39 respiratory tract (M. Costigan, 2001). Because of their important impact on human health, it is  
40 necessary to improve the understanding of the processes responsible for trace elements  
41 release and mobilization.

42 The mobility of arsenic in sedimentary environments has been studied in previous  
43 investigations, because high As concentration in drinking water is particularly common in arid  
44 or semi-arid regions (Robertson, 1989; Wyatt et al., 1998; Levy et al., 1999; Mahlkecht et al.,  
45 2004, Farooqi et al., 2007; Currell et al., 2011, Wang et al., 2018; Yang et al., 2018). The  
46 desorption from Fe-(hydr)oxides was identified as the main process for As release in these  
47 areas under oxidizing environments. In the Pampean aquifer, the origin of As, F, Ba, Sr, and V,  
48 has been widely studied. Many authors attributed the high concentration of these elements  
49 with the presence of volcanic glasses (Nicolli et al., 1989; Smedley et al., 2002; Kruse and  
50 Ainchil, 2003; García et al., 2012; Auge, 2014). Other studies attributed the elevated

51 concentration of trace elements to the process of desorption from Al/Fe/Mn oxides (Smedley  
52 and Kinniburgh, 2002; Bhattacharya et al., 2006; Gomez et al., 2009). Nevertheless, volcanic  
53 glass shards are generally present in a homogeneous proportion in the Pampean sediments,  
54 whereas the concentrations of As, F and other trace elements show high variability throughout  
55 the territory (Blanco et al., 2012). For this reason, it is believed that other mechanisms could  
56 control the mobility of those elements in the groundwater.

57         The ability of calcite ( $\text{CaCO}_3$ ) to retain inorganic contaminants has been described by  
58 many authors (Comans and Middelburg, 1987; Reeder, 1996; Tesoriero and Pankow, 1996;  
59 Cheng et al., 1999; Pokrovsky and Schott, 2002; Roman-Ross et al., 2003; Stipp et al., 2003;  
60 Renard et al., 2015). The uptake of contaminants in calcium carbonates can occur via  
61 adsorption on solid surface or coprecipitation reactions. Calcite has been shown to be capable  
62 of retaining such trace elements, retarding their transport, and thus plays an important role in  
63 the migration of contaminants in natural environments (Zachara et al., 1991; Stipp et al., 1992;  
64 Paquette and Reeder, 1995; Elzinga et al., 2002; Rouff et al., 2004). As banks of calcrete are  
65 extensively present in the Pampean sediments, adsorption or coprecipitation with calcite could  
66 explain most, or part, of the variability of As, F, V, Sr and Ba in the Pampean aquifer.

67         In the Chaco-Pampean plain of Argentina, the shallowest groundwater is contained in a  
68 sedimentary deposit of aeolian origin, which is one the most important sources of water  
69 supply for water to the population, agriculture and industry, and contributes to more than 60%  
70 of the country's gross national product (Schulz and Castro, 2003). The quality of the water  
71 from this reservoir depends on the hydrological balance and the interaction with the materials  
72 that constitute this aquifer. The quality of groundwater for drinking purposes varies greatly  
73 due to the presence of inorganic contaminants such as arsenic, fluoride, and other trace  
74 elements such as vanadium, strontium, and barium (Nicolli et al., 1989; Smedley et al., 2002).  
75 The negative effect of the consumption of water with high content of arsenic in this region is

76 well known (Hopenhayn-Rich et al., 1996; Bardach et al., 2015). In the province of Buenos  
77 Aires, arsenic concentration ranges from 23 to 289  $\mu\text{g.l}^{-1}$  (Al Rawahi et al., 2015) and the  
78 fluoride concentration is approximately 1.0  $\text{mg.l}^{-1}$  (Kruse and Ainchil, 2003; Martínez et al.,  
79 2012; Calvi et al., 2016). In the central arid area of the country, the concentrations of arsenic  
80 and fluoride can be as high as 4.8  $\text{mg.l}^{-1}$  (Bundschuh et al., 2004), and 28  $\text{mg.l}^{-1}$  respectively  
81 (Smedley et al., 2002). In this area, the barium and vanadium concentrations are  
82 approximately 45  $\mu\text{g.l}^{-1}$  and 50  $\mu\text{g.l}^{-1}$ , respectively (Smedley et al., 2002). The concentrations of  
83 these elements exceed the WHO guidelines values in many places (As: 10  $\mu\text{g.l}^{-1}$ ; F: 1.5 $\mu\text{g.l}^{-1}$ ),  
84 presenting risks for human health and limiting the use of groundwater resources (Nicolli et al.,  
85 1989; Bundschuh et al., 2000; Smedley et al., 2000; Fiorentino et al., 2007; Smedley et al.,  
86 2008; Nicolli et al., 2012a; Nicolli et al., 2012b). Whereas barium and strontium are present in  
87 solution as  $\text{Ba}^{2+}$  and  $\text{Sr}^{2+}$  cations, vanadium is generally found in solution as vanadate anions  
88 ( $\text{HVO}_4^{2-}$ ,  $\text{H}_2\text{VO}_4^-$ ), (Al Rawahi, 2016). Arsenic can be present in four oxidation states (-III, 0, + III,  
89 + V) but in the studied hydrological system, it is most commonly found as As (III) ( $\text{H}_3\text{AsO}_3$  or  
90  $\text{H}_2\text{AsO}_3^-$ ) and As (V), ( $\text{H}_2\text{AsO}_4^-$  or  $\text{HAsO}_4^{2-}$ ). The As (V) form is predominant at neutral and alkaline  
91 pH (Smedley et al., 2001). Those inorganic forms of arsenic (As(III) and As(V)) are highly toxic  
92 and mobile in the environment (Smedley and Kinniburgh, 2001; Jang et al., 2016).

93         Since the groundwater resources of the Pampean aquifer are threatened by the high  
94 toxicity of trace elements, it is important to improve the knowledge of their mobilization in  
95 this hydrologic system. In the present study, the putatively important role played by calcrete  
96 for the mobility of trace elements is investigated. Though the chemical composition of the  
97 water of the Pampean aquifer is commonly considered based on a thermodynamic equilibrium  
98 approach (Garrels and Christ, 1965; Glok Galli et al., 2014), it has been demonstrated in a  
99 previous paper that this assumption is questionable for some specific solid phases (Vital et al.,  
100 2018). To go beyond the thermodynamic equilibrium approach, flow-through experiments of  
101 interactions of loess and calcrete with water have been performed and coupled to reactive



102 transport simulations to identify the processes involved in the release of trace elements into  
103 the solution. In addition, while our previous study focused on the release of major elements,  
104 the present study aims at unraveling the source of trace elements released during the flow-  
105 through experiment with calcrete and loess samples.

## 106 **DESCRIPTION OF THE STUDY SITE**

107           The association of sediments occupying a surface area of more than one million square  
108 kilometers is known as the Pampean aquifer (Auge et al., 2002; Auge, 2008). The term  
109 "Pampean sediments" is an informal term and includes the Quaternary aeolian deposits of the  
110 Pampean region, consisting mainly of sand, silt, clay (Frenguelli and Teruggi, 1955). The  
111 sediments of the Pampean aquifer are considered as a formation of loess type. Unlike the  
112 "typical" loess, loess in Argentina has high contents of aluminosilicates and volcanic glass  
113 (Tricart, 1973; Pye, 1995; Zárate, 2003). In general, its composition is homogeneous, and most  
114 of its components originate from volcanic eruptions (Teruggi, 1957; Tricart, 1973). Calcareous  
115 formations occur as concretions and / or banks. Where the calcification is intense, banks of  
116 calcium carbonates result in sedimentary structures of the type of calcrete, locally  
117 denominated "tosca" (Sayago et al., 2001). The Pampean loess composition reveals 2 to 4% of  
118 calcium carbonate as calcite (Teruggi, 1993), mostly located in the upper part of the aquifer.  
119 Calcretes are widely abundant and common in the Pampean sediments, being well distributed  
120 superficially and at different depths. Calcrete is typical of the study site, forming continuous  
121 layers that have been related to paleo-surfaces (Teruggi et al., 1973), occupying the top of the  
122 hills. The calcretes may have formed over periods of several thousand years and are an  
123 indicator of semi-arid conditions (Zárate and Fasano, 1989). Calcrete layers are particularly  
124 abundant in the East of the Buenos Aires province, typically at a depth of around 1 m below  
125 ground level. This has resulted in the development of a largely flat-lying plain. This has been  
126 well described by Zárate and Folguera (2009) quoting original observations done by Charles

127 Darwin (Darwin, 1846). The hydrological conditions in the region are characterized by average  
128 annual precipitations around 900 mm, and a groundwater recharge estimated at 15% of total  
129 precipitation (Quiroz Londoño et al., 2012). The mean pH of the Pampean groundwater in the  
130 studied area is 7.15 (Quiroz-Londoño et al., 2008).

## 131 **MATERIALS AND METHODS**

### 132 **1. Sample collection and mineralogical characterization**

133 Samples of loess and calcrete were collected at an outcrop in the area of Mar del Plata,  
134 in the province of Buenos Aires, Argentina (38°05'12.7"S 57°38'57.1"W), (Figure 1). The area of  
135 sampling was chosen as being a representative area of the mineralogical composition of the  
136 Pampean aquifer in this sector of the Pampa plain. The outcrop includes both loess-like and  
137 calcrete sediments which were collected from a non-saturated zone with the same  
138 sedimentary composition as the Pampean aquifer. The samples were characterized in previous  
139 studies (Vital et al., 2016 ; Vital et al., 2018) using X-ray diffraction (XRD) coupled to Rietveld  
140 refinement and scanning electron microscopy coupled to energy dispersive X-ray spectroscopy  
141 (SEM/EDS). The analysis of the particle size distribution (PSD) by sieving revealed that loess is  
142 composed of 23 % of medium sand (0.25–0.5 mm), 15 % of fine sand (125–250 µm), 25% of  
143 very fine sand (62.5–125 µm) and 37 % of pelites (silt and clay, 0.997–62.5 µm). Calcrete  
144 samples were also collected in other areas of the province of Buenos Aires (Otamendi, Tandil  
145 and Tres Arroyos) in order to check the representativeness of the results obtained for As.

### 146 **2. Flow-through experiments**

147 The experiments were designed to monitor and measure the release of major and  
148 trace elements in the outflowing solution, as a function of reaction time with the solid samples  
149 of loess and calcrete (Figure 2). Continuous flow-through reactors simulate the conditions of  
150 an open geochemical system. The experiments were carried out using the set-up designed by

151 Cama et al. (2000). The Teflon-based continuous flow reactor of known volume of 21.2 cm<sup>3</sup> was  
152 placed on a magnetic stir plate at room temperature. The solid samples of either loess or  
153 calcrete powders were introduced in the reactor. Through this reactor, deionized milliQ water  
154 (pH = 5.7) was continuously injected at a determined flow rate of 5 ml.min<sup>-1</sup>. In this study, the  
155 objective of the experiment was to monitor the total release of the trace elements by the  
156 calcrete and the loess samples. Thus, pure milliQ water was used as a stock solution, to ensure  
157 that the input water is free of the trace elements that are under study. Importantly, the use of  
158 milliQ water is not intended to mimic rainwater or groundwater. This simplification was  
159 necessary to unravel the processes responsible for the release of the considered elements.  
160 Once such process are correctly singled out, the extrapolation to different real conditions (i.e.  
161 different rainwater or groundwater compositions) can be easily achieved by using geochemical  
162 modeling software. The solution inside the reactor was continuously stirred so that the  
163 concentrations and the temperature were theoretically homogeneous. The solution was  
164 maintained at far-from-equilibrium conditions with respect to the dissolving phases because of  
165 the continuous replenishment of the solution.

166 The experiment was designed to evidence the differences in elemental release  
167 between samples of loess and calcrete. It was divided into two steps: the first test T1 and the  
168 second test T2, in order to observe if the targeted elements are quickly and uniquely released  
169 to the solution over T1 (corresponding either to desorption, or to the disappearance of  
170 accessory minerals) or if they are continuously released over T1 and T2 (corresponding to the  
171 congruent dissolution of trace elements that were coprecipitated in major rock-forming  
172 minerals and/or minerals with slow dissolution kinetics). Drying the samples after collecting  
173 them is required to stop the dissolution reaction of the samples, and limit the possible  
174 precipitation of undesired secondary phases formed prior to the onset of the second  
175 experiment. In that way, it was possible to decipher whether the trace elements are adsorbed  
176 on solid particles or coprecipitated as impurities in some minerals. For this purpose, the

177 samples of loess and calcrete were introduced two times in the reactor. First, 2 grams of  
178 powder (loess or calcrete from the various above-mentioned locations) were introduced in the  
179 reactor for 2 hours. Sampling of the outflowing aqueous solution was carried out at the  
180 following duration steps: 1, 3, 5, 10, 15, 20, 30, 45, 60, 90 and 120 minutes. Those collected  
181 aqueous samples correspond to the first test T1. Afterwards, the solid samples were recovered  
182 at the end of the experiments, dried in an oven for 24 hours at 60°C. The dried solid samples  
183 were then put back in the flow-through reactor for two additional hours. The collection of  
184 aqueous samples in the second part of the experiment was carried out using the same  
185 previous time steps. The collected aqueous samples correspond to the second test T2. The  
186 experiments were repeated 3 times for each samples and each location. In all cases, the  
187 aqueous samples were filtered through a 0.45 µm filter and stored at -4°C prior to their  
188 analyses.

### 189 3. Aqueous sample analyses

190 The aqueous solution samples recovered at the reactor outlet, from the experiments  
191 realized with the loess and calcrete samples from the area of Mar del Plata, were analyzed to  
192 quantify the concentration of calcium, sodium, potassium and magnesium by capillary  
193 electrophoresis at the National Atomic Energy Commission (CNEA) laboratory (Buenos Aires,  
194 Argentina) with a Beckman Coulter brand equipment using a 40 cm-long fused silica capillary  
195 with a diameter of 75 µm (25 KV). The background electrolyte (BGE) was composed of a  
196 deimidazole solution of 10 mmol.l<sup>-1</sup>, and acetic acid (40 mmol.l<sup>-1</sup>). BGE was used as a buffer  
197 and is essential to stabilize the electro-osmotic flow and the migration time of the analytes.  
198 Calcium, sodium, potassium and magnesium standard solutions of 0.1, 0.5, 1, 5, 10, and 15  
199 ppm were injected to determine the time after which each element appeared and to obtain  
200 the calibration curve of the peak area vs. the concentration. Sulfate, chloride and fluoride  
201 concentrations of the aqueous samples were measured by high performance liquid

202 chromatography (HPLC) with a Thermo Separation Products, CA, USA team, with a Spectra  
203 SERIES P200 binary pump, and a UV-Vis UV100 detector. An HPLC anion exchange column,  
204 PRP-X100, HAMILTON® and a mobile phase of potassium biphthalate ( $4,5 \text{ mmol.l}^{-1}$ ) were used  
205 at the CNEA laboratory. Standard solutions of 0.5, 1, 2, 5, 10 and 15 ppm of fluorine, sulfate,  
206 and chloride were prepared to establish pattern curves in order to calibrate the concentration  
207 of each anion as a function of the area of the peak. The barium, vanadium, strontium, arsenic  
208 and silica concentrations of the aqueous samples were measured by inductively coupled  
209 plasma atomic emission spectroscopy (ICP-AES) with a Thermo ICAP 6000 brand equipment at  
210 the laboratory of hydrology and geochemistry of Strasbourg (France). In all analyses, pure  
211 milliQ water was used as a blank standard.

212 Arsenic concentrations of the aqueous samples obtained from the experiments T1 and  
213 T2 realized with the calcrete samples from the area of Tandil and Tres Arroyos were  
214 determined by Total reflection X-Ray Fluorescence (TXRF), using a TXRF spectrometer S2  
215 Picofox (Bruker, Germany).

#### 216 4. KIRMAT Modeling

217 Fluorapatite was identified in the loess and calcrete samples (Vital et al, 2018) and  
218 fluorine has been detected as an impurity in the calcrete with concentrations ranging between  
219 approximately  $220 \mu\text{g.g}^{-1}$  (García et al., 2006) and up to  $1500 \text{ mg.kg}^{-1}$  (Limbozzi, 2015).  
220 According to those observations, kinetic modeling was performed to assess the contribution of  
221 fluorapatite and fluoride-bearing calcite to the concentration of fluoride in the aqueous  
222 samples. Kinetic simulations coupled to mass transport were realized with the hydrochemical  
223 and thermo-kinetic code KIRMAT (KInetic Reaction and MAss Transfer), (Gérard et al., 1998). A  
224 phase of calcite with 0.1% of fluoride as an impurity with a solubility identical to that of pure  
225 calcite was added to the KIRMAT thermodynamic database. The concentrations of fluoride  
226 obtained in the flow-through experiments test 1 (T1) and test 2 (T2) with the samples of loess

227 from Mar del Plata, and the samples of calcrete from the four locations, were compared to  
228 dissolution simulations of loess and calcrete containing fluorapatite or F-bearing calcite (0.1%  
229 of fluoride). The BET surface area of each sample from (Vital et al., 2018) was used as well as  
230 kinetic rate laws gathered in Palandri and Kharaka, (2004). Other input parameters for the  
231 simulations include deionized water in equilibrium with atmospheric CO<sub>2</sub> (corresponding to a  
232 starting pH of 5.7), a temperature of 25°C, and a flow rate of 5 ml.min<sup>-1</sup>. The thermodynamic  
233 database used in KIRMAT comes from the THERMODDEM database of the Bureau de  
234 Recherche Geologique et Minière (BRGM - <http://www.brgm.fr/>).

## 235 **RESULTS**

236 To determine the source of trace elements and their relations to major ions, the  
237 evolution of the output concentrations of major and minor elements obtained from the flow-  
238 through experiments conducted with loess and calcrete samples from the area of Mar del  
239 Plata are presented in Table 1 and Figure 3.

### 240 **1. Experiments conducted on loess samples**

241 In the experiment conducted on loess samples, the major ions SiO<sub>2</sub>(aq), Ca<sup>2+</sup>, Na<sup>+</sup>, SO<sub>4</sub><sup>2-</sup>, Cl<sup>-</sup> and  
242 K<sup>+</sup> are released in the solution following each of them a similar tendency, which consists of an  
243 initial peak of ion incorporation after the very first minutes of the experiment in the test T1.  
244 Then, the concentrations of SiO<sub>2</sub>(aq), Ca<sup>2+</sup>, Na<sup>+</sup>, SO<sub>4</sub><sup>2-</sup>, Cl<sup>-</sup> and K<sup>+</sup> decrease to reach a constant  
245 final value after 120 minutes (TF1). A lower concentration of those ions is measured in T2 but  
246 also starting with an initial peak of release. In detail, the highest concentration of silica (0.24  
247 mmol.l<sup>-1</sup>) was measured in the sample collected during the first minute of contact with loess  
248 (table 1). Subsequently, the silica concentration dramatically decreases to reach 0.04 mmol.l<sup>-1</sup>  
249 all over T1. In the second test(T2), a significant release of silica was observed in the first minute  
250 (0.21 mmol.l<sup>-1</sup>) followed by a very significant decrease. Sodium and chloride ions are released

251 very quickly to the solution, with the highest concentrations reached during the first minute of  
252 T1(3.3 and 21 mmol.l<sup>-1</sup>, respectively). A very significant decrease in the concentrations of these  
253 elements is observed to reach stable values in the first hour of T1(0.2 and 0.01 mmol.l<sup>-1</sup>). Over  
254 the course of T2,the values measured in the samples in the first minute are significantly lower  
255 than the values measured in the first minute of T1 (0.09 and 0.1 mmol.l<sup>-1</sup>). The same trend is  
256 observed for calcium and sulfate ions, with the highest concentrations reached in the first  
257 minutes of T1 of 4.8 mmol.l<sup>-1</sup> and 0.7 mmol.l<sup>-1</sup>.

258 The pH of the outflowing solution follows the patterns observed for the released ions. The pH  
259 of the initial input solution is 5.7. Initially, a fast increase from 5.7 to 6.6 is observed, but then  
260 pH decreases slowly to the initial input value after 180 min. The same behavior was observed  
261 for the TDS.

262 The behavior of trace elements is more complex (Figure3): while the concentration of some  
263 elements such as Sr and V follows a trend that is similar to that of major ions (i.e., initial peak  
264 after one minute in T1 and T2 followed by a decrease and the attainment of a steady-state  
265 concentration), the concentrations of other elements (e.g., Ba, F, As) steadily decrease  
266 throughout T1 and T2. The initial concentration of Sr<sup>2+</sup> reached 8.72 μmol.l<sup>-1</sup> in T1, with a  
267 decrease down to 0.2 μmol.l<sup>-1</sup>, followed by another peak in T2 at 0.3 μmol.l<sup>-1</sup>. The  
268 concentration of vanadium is 0.2 μmol.l<sup>-1</sup> at the beginning of T1 and then, after an initial peak  
269 in T2 (0.07 μmol.l<sup>-1</sup>), the final concentration of V is far below 0.1 μmol.l<sup>-1</sup>. On the other hand,  
270 trace elements such as F<sup>-</sup>, Ba<sup>2+</sup>, and As start with a peak concentration in T1 (0.03 mmol.l<sup>-1</sup>, 0.  
271 51 μmol.l<sup>-1</sup> and 0.027 μmol.l<sup>-1</sup> respectively) to decrease in all T1 and T2, and As concentration is  
272 even below the detection limit in T2. These results provide a first indirect indication that these  
273 elements were either released from specific minor phases enriched in these elements that  
274 were completely dissolved by the end of T2, or that they have been rapidly desorbed from the  
275 solid samples.

276 Further treatment of the data was carried out for the determination of the origin of other  
277 trace elements. While only  $\text{Sr}^{2+}$  is linearly correlated with  $\text{Ca}^{2+}$  release ( $r^2 = 1$ ) (Figure 4), the  
278 concentrations of  $\text{Sr}^{2+}$  and  $\text{Ba}^{2+}$  in the aqueous samples are linearly correlated with that of  $\text{Na}^+$   
279 ( $r^2_{\text{Na/Sr}} = 0.999$  and  $r^2_{\text{Na/Ba}} = 0.96$ ) and  $\text{K}^+$  ( $r^2_{\text{K/Sr}} = 0.93$  and  $r^2_{\text{K/Ba}} = 0.97$ ); (Figure 5). A lack of linear  
280 correlations between V and As concentrations and  $\text{Na}^+$  or  $\text{K}^+$  concentrations can be observed in  
281 Figure 5, as well as no linear correlation between  $\text{Ca}^{2+}$  and  $\text{F}^-$  in T1 ( $r^2 = 0.69$ ) (Figure 6). On the  
282 contrary, a linear correlation is observed between the release of  $\text{F}^-$  and  $\text{Ca}^{2+}$  in the test T2 ( $r^2 =$   
283 0.95)

## 284 **2. Experiments conducted on calcrete samples**

285 In these experiments, the initial pH (5.7) quickly increased to stabilize at values comprised  
286 between 7.6 and 7.9, because of the  $\text{CaCO}_3$  dissolution. These are the typical values of  
287 groundwater at the southeast of the province of Buenos Aires. The variation in concentrations  
288 in T1 and T2 of major ions are presented in Table 1. The highest concentration of calcium ( $0.64$   
289  $\text{mmol.l}^{-1}$ ) was obtained in the first minute of the test T1, and decreased down to  $0.2 \text{ mmol.l}^{-1}$   
290 after 20 minutes of reaction. In the second test, a peak of  $\text{Ca}^{2+}$  appears in the first minute of  
291 reaction ( $0.37 \text{ mmol.l}^{-1}$ ). A peak of sodium ( $3.3 \text{ mmol.l}^{-1}$ ) and chloride ( $21 \text{ mmol.l}^{-1}$ ) is observed  
292 in the first minute of the experiment and then the concentrations stabilized below  $0.5 \text{ mmol.l}^{-1}$   
293 and  $0.1 \text{ mmol.l}^{-1}$  respectively. In the test T2, a very similar trend is observed for the two  
294 elements. Similar trends were observed for  $\text{SiO}_2(\text{aq})$  and  $\text{SO}_4^{2-}$ .

295 The experiments conducted with calcrete exhibited large release of strontium and barium  
296 during the first minutes of reaction in the first test (T1) and second test (T2), followed by a  
297 progressive decrease in the release rate of these ions during the subsequent hours (Figure 3).  
298 Of note, the maximum concentrations of  $\text{Sr}^{2+}$  and  $\text{Ba}^{2+}$  at the beginning of T2 are equivalent to  
299 those reached at the beginning of T1. Conversely, vanadium concentration peaks to a higher  
300 value in the first test ( $0.9 \text{ } \mu\text{mol.l}^{-1}$ ) compared to the second test ( $0.1 \text{ } \mu\text{mol.l}^{-1}$ ). Arsenic is



301 detected in T1 ( $0.027 \mu\text{mol.l}^{-1}$ ) and only at the beginning of T2 ( $0.013 \mu\text{mol.l}^{-1}$ ). A linear relation  
302 was evidenced between the concentration of calcium and the trace elements  $\text{Ba}^{2+}$  ( $r^2 = 0.97$ ),  
303 As ( $r^2 = 0.93$ ), and  $\text{Sr}^{2+}$  ( $r^2 = 0.99$ ), (Figure 7a), and to a lesser extent, V ( $r^2 = 0,84$ ). No linear  
304 relationship between  $\text{Ca}^{2+}$  and  $\text{F}^-$  concentrations was evidenced in T1. Conversely, the linear  
305 relationship was retrieved in T2 ( $r^2 = 0,86$ ), (Figure 7b).

### 306 **3. Confirmation of the control of As mobilization by calcite contained in calcrete**

307 Flow-through experiments were repeated with calcrete from three other places of the  
308 province of Buenos Aires: Otamendi, Tres Arroyos, and Tandil. Arsenic concentrations were  
309 measured by TXRF, which is a method less sensitive than ICP-AES. Semi-quantitative values  
310 were obtained, indicating that arsenic was detected in almost all the aqueous samples (Table  
311 2). In the first and second tests, the concentration ranged from  $0.002$  to  $0.005 \text{ mg.l}^{-1}$  ( $0.026$   
312  $\mu\text{mol.l}^{-1}$  to  $0.067 \mu\text{mol.l}^{-1}$ ). This experiment showed that As is most certainly incorporated into  
313 calcite, as supported by the linear correlation between  $\text{Ca}^{2+}$  and As previously reported in  
314 Figure 7a.

### 315 **4. Unravelling the source of fluoride using reactive transport modeling**

316 The fluoride concentrations measured in T1 and T2 conducted with loess and calcrete were  
317 compared with the outputs of simulations of sediment (calcrete or loess) dissolution  
318 containing F-calcite and fluorapatite (Figure 8). Fluorapatite was previously detected by SEM  
319 observations reported in Vital et al. (2018) but could not be identified by XRD. Because it was  
320 estimated that the detection limit of our XRD was  $\sim 2 \text{ wt. } \%$ , we ran the kinetic simulations  
321 using this value as an upper bound for fluorapatite content in the solid sample. Also, calcite  
322 containing  $0.1 \text{ wt. } \%$  of F was added (calcite represent  $>90\%$  of the weight of the calcrete  
323 sample, and  $1-2\%$  of the loess sample). Following Kitano and Okumura (1973),  $0.1 \text{ wt. } \%$  is the

324 maximum concentration of F that can be incorporated into calcite. We used this value as an  
325 upper bound for the F content of calcite.

326 Figure 8 shows the results of the fluoride concentrations obtained in T1 and T2 flow-through  
327 experiments for the loess sample. As can be seen, the model successfully predicts the  
328 concentration of fluoride measured by the end of experiment T2. It further reveals that calcite  
329 is the main contributor to this agreement, as testified from the simulation performed with 0  
330 wt. % of F-calcite and 2 wt. % of fluorapatite. Nevertheless, the first peak in T1 could not be  
331 fitted, which is an indirect evidence for a two-step process: (i) desorption of F at the beginning  
332 of the experiment T1 (not taken into account in the simulation), and (ii) continuous release  
333 from F-bearing phases.

334 A similar approach was used for calcrete from Mar del Plata, Otamendi, Tandil and Tres  
335 Arroyos flow-through experiments. The simulations were conducted with 2 wt. % of  
336 fluorapatite and considering F-bearing calcite instead of pure calcite (Figure 8b). The outputs  
337 of the simulations are in good agreement with the concentration plateau observed in T2, but,  
338 again, the initial peak of fluoride release at the beginning of T1 could not be fitted.

## 339 **DISCUSSION**

### 340 **1. Experiments conducted on loess samples**

341 An initial peak of major ion such as  $\text{SiO}_2(\text{aq})$ ,  $\text{Na}^+$ ,  $\text{Cl}^-$ ,  $\text{Ca}^{2+}$  is systematically observed in the  
342 flow-through experiments of loess in test 1. This may result from the rapid dissolution of the  
343 finest particles of the primary rock forming minerals (e.g., Schott et al., 1981). In T2 series,  
344 these elements are still released to the solution, with a steady-state concentration close to the  
345 concentration reached at the end of T1. Not surprisingly, these results indicate that these  
346 elements must have been released by mineral phases that were not completely consumed by  
347 the end of the T1, i.e., most likely the dissolution of primary rock-forming minerals. In a

348 previous study (Vital et al., 2018), we showed that the release of major ions from loess is  
349 related to the presence of minerals such as quartz, albite and accessory minerals such as  
350 halite, gypsum and calcite. An initial peak of strontium, vanadium, barium, fluoride and arsenic  
351 is also observed in T1. The concentrations of those elements decrease all along T1 and T2.

352 The presence of vanadium, strontium, barium and arsenic in groundwater has been related to  
353 loess deposits (Farías et al., 2003; Fiorentino et al., 2007; Nicolli et al., 2012a), mainly due to  
354 the release from volcanic glass shards and Al/Fe oxides (Steinhauser and Bichler, 2008; Nicolli  
355 et al., 2010; Nicolli et al., 2012a; Nicolli et al., 2012b; Bia et al., 2015; Barranquero et al., 2017;  
356 Alvarez and Carol, 2018), which could explain the behavior of the trace elements in the flow-  
357 through experiments T1 and T2 conducted on loess. The desorption of As and F from Fe/Mn  
358 oxides has been mentioned in many other studies focused on aquifers in China (Currell et al.,  
359 2011), or Korea (Kim et al., 2012), and Argentina (Smedley et al., 2002; Smedley et al.,  
360 2005; Bhattacharya et al., 2006; Borgnino et al., 2013). Currell et al., 2011 showed that  
361 increasing the duration of the interaction between water and loess samples generally did not  
362 result in an increase in F or As concentrations in solution and indicated that these ions are  
363 most likely mobilized by de-sorption rather than dissolution of F- or As-bearing minerals. Our  
364 results with the loess sample of the area of Mar del Plata are consistent with this previous  
365 study, suggesting that the rapid release of As could be the consequence of the desorption from  
366 those solid surfaces.

367 The results also show that only Sr is linearly correlated with Ca release. Vital et al., 2018  
368 showed that the loess samples could contain up to 2% of calcite. Therefore, the strontium was  
369 likely coprecipitated with calcite, and its release to the solution results from calcite dissolution.  
370 In addition, the concentrations of  $Sr^{2+}$  and  $Ba^{2+}$  in the aqueous samples are linearly correlated  
371 with that of  $Na^+$  and  $K^+$ . The correlation of  $Ba^{2+}$  and  $Sr^{2+}$  with  $Na^+$  and  $K^+$  could also suggest that  
372 these trace elements were incorporated into the main rock-forming minerals of the loess

373 sample (feldspars). Conversely, the absence of linear correlations between V and As  
374 concentrations and Na<sup>+</sup> or K<sup>+</sup> concentrations supports the assumption that these trace  
375 elements were not released from the congruent dissolution of feldspars. Instead, it is  
376 suggested that they were carried by minor phases that have almost disappeared by the end of  
377 the experiment T2. Furthermore, Nicolli et al., (1989), Bhattacharya et al. (2006), Fiorentino et  
378 al. (2007), Heredia and Cirelli (2009), Puntoriero et al. (2015), showed that V is strongly  
379 correlated with As in groundwaters in the Pampean Region. This result indicates that those  
380 elements may have similar sources, mobilization and transport processes and could be mainly  
381 desorbed from Al/Mn oxides.

382 Finally, no linear correlation between Ca and F was evidenced in the T1 test, questioning the  
383 possibility that F was released congruently from a putative F-bearing calcite. Instead, the  
384 mechanism of fluoride release may be the rapid desorption from the particle's surface.  
385 Conversely, a linear correlation can be observed between Ca and F concentrations in the T2  
386 test. Therefore, it is likely that the loess sample contains a second pool of fluoride, which might  
387 have been released through the congruent dissolution of a Ca-rich phase, such as the putative  
388 F-bearing calcite. The ability of calcite to be either a substrate for fluoride  
389 adsorption/desorption, or to incorporate fluoride during the course of its precipitation has  
390 been supported by the works of Kitano and Okumura (1973); Turner et al. (2005); Budyanto et  
391 al. (2015); Padhi and Tokunaga (2015).

## 392 **2. Experiments conducted on calcrete samples**

393 Calcium and trace elements were released all over the experiments conducted on calcrete,  
394 with an initial peak at the beginning of each test T1 and T2. The observed linear correlation  
395 between the concentration of calcium and the trace elements Ba, As, Sr and V, suggests that  
396 these elements were coprecipitated in calcite and their release results from calcite dissolution.  
397 This suggestion is supported by the work of Dietrich et al. (2016), who showed that carbonates

398 were the main As-bearing minerals in the carbonate-rich unsaturated zone from a large plain  
399 environment (Pampean plain, Argentina). Moreover, Renard et al. (2015) showed that  
400 As(V) was mostly incorporated in the calcite structure. When calcite dissolves, these elements  
401 are released stoichiometrically to the solution. In numerous studies, it has been demonstrated  
402 that calcite is able to retain trace elements, delaying their transport (Zachara et al., 1991; Stipp  
403 et al., 1992; Paquette and Reeder, 1995; Elzinga and Reeder, 2002; Rouff et al., 2004). The  
404 results obtained in the present work confirm the conclusions of these previous studies. An  
405 absence of linear relationship between Ca and F concentrations in the T1 test conducted with  
406 calcrete was observed, while this correlation was evidenced in the second T2 test. These latter  
407 results are very similar to those previously discussed for loess: At the beginning of T1, the main  
408 mechanism is F desorption from minerals surface (Kumar et al., 2016). The second mechanism,  
409 which prevails after the F on particles surface is totally desorbed, could be the release of  
410 fluoride that was incorporated in calcite.

411 **3. Confirmation of the control of trace elements mobilization by calcite contained**  
412 **in calcrete**

413 A significant difference was observed in the behavior of the trace elements released from loess  
414 or calcrete samples. The highest concentrations of vanadium, barium and arsenic have been  
415 measured for the experiments conducted with loess. These elements were released quickly to  
416 the solution in the first minute of T1 before decreasing sharply, while for calcrete, a  
417 continuous release is observed, and these trace elements are still released to the solution over  
418 the course of T2. This behavior was observed in four location of the province of Buenos Aires.  
419 The mechanisms of trace elements release from volcanic glass shards or Fe/Al/Mn oxides  
420 mentioned above could explain the higher concentration of trace elements in the aqueous  
421 samples collected for the experiments conducted with loess.

422 Conversely, trace elements may have been coprecipitated in calcite, which would explain their  
423 continuous release to the solution throughout the experiments conducted with calcrete. The  
424 experiments conducted with calcrete samples from different location (Tandil, Otamendi, Tres  
425 Arroyos) show that the release of trace elements from calcrete may apply throughout the  
426 Buenos Aires province. Importantly, the present results demonstrate that calcium carbonate  
427 may play a prevailing role in controlling the trace elements distribution for the study site. To  
428 the best of our knowledge, this aspect had never been proposed before in this area.  
429 Depending on the solution composition, calcium carbonates can therefore act as a sink for As if  
430 precipitation occurs, or as a source during dissolution. Alexandratos et al. (2007) suggested that  
431 arsenates are substituted in carbonate sites of calcite in most of the calcrete that is present in  
432 the Pampean aquifer. Sørensen et al. (2008) measured that the adsorption of arsenate increases with  
433 decreasing alkalinity, indicating a competition between arsenate and (bi)carbonate for  
434 sorption sites. These authors also observed that the mobility of arsenate in calcite bearing  
435 aquifers is greatly reduced due to sorption on calcite, whereas sorption on calcite in aquifers  
436 with low calcite content affects the mobility of arsenate to a lesser extent. Another study  
437 (Romero et al., 2004) focused on the carbonate-rich aquifer at Zimapán, México showed that  
438 carbonates play an important role in As mobility, and proved the high capacity of As(V)  
439 retention from this material. It was also shown that at alkaline pH (between 7 and 9), the  
440 carbonate-rich sample had a higher retention capacity of As.

441 Considering the presence of thick layers of calcrete and groundwater pHs around 7.5 to 8.0, it  
442 is possible to conclude that the coprecipitation and desorption from calcretes are factors  
443 controlling the As and other trace elements mobility and distribution in the aquifer. The  
444 experimental results showed that calcrete dissolution can be the most important source for As  
445 over long time periods, when the solution is undersaturated with respect to calcite. On the  
446 contrary, when the solution is supersaturated with respect to calcite, it can precipitate with  
447 trace-elements and act as a sink for these elements. It is expected that the calcite saturation

448 index of water samples could be considered as a proxy of As contents for some zones, as  
449 shown by Calvi et al. (2016), who reported a correlation between calcite supersaturation areas  
450 and low fluoride concentrations.

#### 451 **4. Unravelling the source of fluoride using reactive transport modeling**

452 The results of the KIRMAT modeling showed that the neither fluorapatite nor F-calcite  
453 dissolution can account for the initial peak of F observed in T1 for loess and calcrete  
454 experiments, leaving F desorption as the best explanation for the observed F release when the  
455 sample is put in contact with water for the first time. Of note, several studies indicated that  
456 fluorine comes from surface desorption, as it was found adsorbed on calcite particles (Turner  
457 et al., 2005), iron oxides (Borgnino et al., 2013), or associated with volcanic glasses (Bundschuh  
458 et al., 2004; Bhattacharya et al., 2006; Nicolli et al., 2012a; García et al., 2014). These  
459 observations are in good agreement with the very fast release of fluorine to the solution and  
460 further suggest that when the sample was put in contact with water for the first time, the  
461 initial mechanism of F release is surface desorption.

462 Interestingly, the concentration of fluoride measured in the T2 for both loess and calcrete  
463 samples match the simulations of KIRMAT. This result confirms that in T2, a second mechanism  
464 of F release occurs and is most probably the release from F-bearing minerals such as  
465 fluorapatite and F coprecipitated in calcite. Therefore, we suggest that the two mechanisms of  
466 F release (desorption and dissolution from calcite and fluorapatite) may superimpose. Again,  
467 this confirms that calcrete plays an important role in the release of trace elements.

#### 468 **CONCLUSION**

469 In this study, flow-through experiments associated to kinetic modeling were used in order to  
470 assess the specific role of calcite in the control of the mobility of trace elements in the  
471 Pampean aquifer. Samples of loess and calcrete from different areas of the province of Buenos

472 Aires (Mar del Plata, Tandil, and Tres Arroyos) were collected. In the experiments, the solid  
473 samples were first reacted with water in a flow-through set-up, dried, and then put again in  
474 contact with water. The chemical composition of the aqueous solution varied with the type of  
475 solid sample reacting (loess or calcrete). Regarding experiments conducted with loess, arsenic  
476 and other trace elements (V, Ba, Sr) were rapidly released during the first minute of reaction,  
477 likely due to their desorption from solid particles in loess. These observations agree with the  
478 results of other studies suggesting that the original source of those trace elements could be  
479 the volcanic glass or the Al/Fe/Mn oxides shards present in the loess sample. On the contrary,  
480 regarding experiments conducted with calcrete, those trace elements were released to the  
481 solution for several minutes, but also in the second experiment performed with the dried  
482 samples recovered from the first experiment. It has been shown in this work that arsenic,  
483 barium, vanadium and strontium have a strong correlation with Ca during the first part of the  
484 experiment, suggesting that they are released to the solution as a result of calcite dissolution.  
485 This work shows that calcite plays an important role in the migration of inorganic  
486 contaminants such as arsenic in the environment. The mobilization of contaminants from  
487 calcium carbonates can occur by desorption from the solid surface or by dissolution of the  
488 coprecipitated elements. In the Pampean aquifer, those trace elements can be coprecipitated  
489 in the calcrete banks and can be re-mobilized by calcite dissolution as a result of variation in  
490 physicochemical changes in the groundwater (i.e. pH, saturation index). For both loess and  
491 calcrete samples, fluorine release occurred through two different mechanisms. In a first step,  
492 the fluoride that is most likely adsorbed to the surface of the particles is released to the  
493 solution. Afterwards, fluorine coprecipitated in calcite is released to the solution. The use of  
494 reactive transport modeling allowed validating this model. In the future, it would be  
495 interesting to expand this study on loess and calcrete from different locations and different  
496 depths of the very great territory of Argentina. Because it was demonstrated in this study that  
497 trace elements adsorption/desorption and precipitation/dissolution from calcrete are



498 important processes impacting the groundwater chemistry, it would be necessary to include  
499 them in the geochemical simulations. This would allow to improve the knowledge of the  
500 mobilization and distribution of As and other trace elements in groundwater.

501

502 **Acknowledgements:**

503 The authors are thankful to the National Agency for Science and Technology Promotion  
504 (ANPCyT, PICT 2014 N°1529) which supported this study financially and to the National  
505 Scientific and Technical Research Council (CONICET). We also acknowledge the Mincyt-ECOS  
506 project for supporting international collaboration between the ICGyC/IIMyC in Argentina and  
507 the LHyGes in France. The authors are also thankful to Dr. Carlos Ayora and Dr. Jordi Cama  
508 (IDÆA, CSIC) for providing the Flow-through reactor and to Mr. G. Bernava for the chemical  
509 analyses. The authors thank Gilles Morvan (LHyGeS), and René Boutin (LHyGeS) for performing  
510 MEB, providing supplementary data and helping with ICP-AES measurements, respectively.  
511 This work has benefited from the constructive comments and insightful suggestions of 3  
512 anonymous reviewers who are warmly thanked.

514

515

516 Agusa, T., Trang, P. T. K., Lan, V. M., Anh, D. H., Tanabe, S., Viet, P. H., & Berg, M. (2014).  
517 Human exposure to arsenic from drinking water in Vietnam. *Science of the total*  
518 *Environment*, 488, 562-569. doi: <https://doi.org/10.1016/j.scitotenv.2013.10.039>

519 Al Rawahi, W., Marcilla, A., & Ward, N. (2015). Arsenic Speciation Analysis of Ground Waters  
520 in Southern La Pampa and Buenos Aires Proviinces, Argentina.

521 Al Rawahi, W. A. (2016). Vanadium, arsenic and fluoride in natural waters from Argentina and  
522 possible impact on human health (Doctoral dissertation, University of Surrey (United  
523 Kingdom)).

524 Alexandratos, V. G., Elzinga, E. J., & Reeder, R. J. (2007). Arsenate uptake by calcite:  
525 macroscopic and spectroscopic characterization of adsorption and incorporation  
526 mechanisms. *Geochimica et Cosmochimica Acta*, 71(17), 4172-4187. doi:  
527 <https://doi.org/10.1016/j.gca.2007.06.055>

528 Alvarez, M. d. P., & Carol, E. (2018). Geochemical occurrence of arsenic, vanadium and fluoride  
529 in groundwater of Patagonia, Argentina: Sources and mobilization processes. *Journal*  
530 *of South American Earth Sciences*. doi: <https://doi.org/10.1016/j.jsames.2018.10.006>

531 Auge, M. (2008). Agua subterránea, deterioro de calidad y reserva. *Facultad de Ciencias*  
532 *Exactas y Naturales (UBA)*. [http://sedici.unlp.edu.ar/bitstream/handle/10915/15908/  
533 Documento\\_completo.pdf?sequence=1&isAllowed=y](http://sedici.unlp.edu.ar/bitstream/handle/10915/15908/Documento_completo.pdf?sequence=1&isAllowed=y)

534 Auge, M. (2014). *Arsenic in the groundwater of the Buenos Aires province, Argentina*. Paper  
535 presented at the One Century of the Discovery of Arsenicosis in Latin America (1914-  
536 2014) As2014: Proceedings of the 5th International Congress on Arsenic in the  
537 Environment, May 11-16, 2014, Buenos Aires, Argentina.

538 Auge, M. P., Hernández, M. A., & Hernández, L. (2002). *Actualización del conocimiento del*  
539 *acuifero semiconfinado Puelche en la provincia de Buenos Aires, Argentina*. Paper  
540 presented at the XXXII IAH & VI ALHSUD Congress. Actas.

541 Bardach, A. E., Ciapponi, A., Soto, N., Chaparro, M. R., Calderon, M., Briatore, A., Cadoppi, N.,  
542 Tassara, R., & Litter, M. I. (2015). Epidemiology of chronic disease related to arsenic in  
543 Argentina: A systematic review. *Science of the total Environment*, 538, 802-816. doi:  
544 <https://doi.org/10.1016/j.scitotenv.2015.08.070>

545 Barranquero, R. S., Varni, M., Vega, M., Pardi, R., & Ruiz de Galarreta, A. (2017). Arsenic,  
546 fluoride and other trace elements in the Argentina Pampean plain. *Geologica acta*,  
547 15(3), 0187-0200. doi: 10.1344/GeologicaActa2017.15.3.3

548 Bhattacharya, P., Claesson, M., Bundschuh, J., Sracek, O., Fagerberg, J., Jacks, G., Martin, R. A.,  
549 Storniolo, A. d. R., & Thir, J. M. (2006). Distribution and mobility of arsenic in the Rio  
550 Dulce alluvial aquifers in Santiago del Estero Province, Argentina. *Science of the total*  
551 *Environment*, 358(1), 97-120. doi: <https://doi.org/10.1016/j.scitotenv.2005.04.048>

552 Bia, G., Borgnino, L., Gaiero, D., & García, M. G. (2015). Arsenic-bearing phases in South  
553 Andean volcanic ashes: Implications for As mobility in aquatic environments. *Chemical*  
554 *Geology*, 393, 26-35. doi: <https://doi.org/10.1016/j.chemgeo.2014.10.007>

555 Blanco, M. d. C., Paoloni, J. D., Morrás, H., Fiorentino, C., Sequeira, M. E., Amiotti, N. N., Bravo,  
556 O., Diaz, S., & Espósito, M. (2012). Partition of arsenic in soils sediments and the origin  
557 of naturally elevated concentrations in groundwater of the southern pampa region  
558 (Argentina). *Environmental Earth Sciences*, 66(7), 2075-2084. doi:  
559 <https://doi.org/10.1007/s12665-011-1433-x>

560 Borgnino, L., Garcia, M., Bia, G., Stupar, Y., Le Coustumer, P., & Depetris, P. (2013).  
561 Mechanisms of fluoride release in sediments of Argentina's central region. *Science of*

562           the           total           Environment,           443,           245-255.           doi:  
563           https://doi.org/10.1016/j.scitotenv.2012.10.093

564 Budyanto, S., Kuo, Y.-L., & Liu, J. (2015). Adsorption and precipitation of fluoride on calcite  
565 nanoparticles: a spectroscopic study. *Separation and Purification Technology*, 150,  
566 325-331. doi: https://doi.org/10.1016/j.seppur.2015.07.016

567 Bundschuh, J., Bonorino, G., Viero, A., Albouy, R., & Fuertes, A. (2000). *Arsenic and other trace*  
568 *elements in sedimentary aquifers in the Chaco-Pampean Plain, Argentina: Origin,*  
569 *distribution, speciation, social and economic consequences.* Paper presented at the  
570 Arsenic in Groundwater of Sedimentary Aquifers, Pre-Congress Workshop, 31st  
571 Internat. Geol. Cong., Rio de Janeiro, Brazil.

572 Bundschuh, J., Farias, B., Martin, R., Storniolo, A., Bhattacharya, P., Cortes, J., Bonorino, G., &  
573 Albouy, R. (2004). Groundwater arsenic in the Chaco-Pampean plain, Argentina: case  
574 study from Robles county, Santiago del Estero province. *Applied Geochemistry*, 19(2),  
575 231-243. doi: https://doi.org/10.1016/j.apgeochem.2003.09.009

576 Calvi, C., Martinez, D., Dapeña, C., & Gutheim, F. (2016). Abundance and distribution of  
577 fluoride concentrations in groundwater: La Ballenera catchment, southeast of Buenos  
578 Aires Province, Argentina. *Environmental Earth Sciences*, 75(6), 534. doi:  
579 https://doi.org/10.1007/s12665-015-4972-8

580 Cama, J., Ganor, J., Ayora, C., & Lasaga, C. A. (2000). Smectite dissolution kinetics at 80 C and  
581 pH 8.8. *Geochimica et Cosmochimica Acta*, 64(15), 2701-2717. DOI: 10.1016/S0016-  
582 7037(00)00378-1

583 Chakraborti, D., Rahman, M. M., Ahamed, S., Dutta, R. N., Pati, S., & Mukherjee, S. C. (2016).  
584 Arsenic groundwater contamination and its health effects in Patna district (capital of  
585 Bihar) in the middle Ganga plain, India. *Chemosphere*, 152, 520-529. doi:  
586 https://doi.org/10.1016/j.chemosphere.2016.02.119

587 Chappells, H., Parker, L., Fernandez, C. V., Conrad, C., Drage, J., O'Toole, G., Campbell, N., &  
588 Dummer, T. J. (2014). Arsenic in private drinking water wells: an assessment of  
589 jurisdictional regulations and guidelines for risk remediation in North America. *Journal*  
590 *of water and health*, 12(3), 372-392. doi: https://doi.org/10.2166/wh.2014.054

591 Cheng, L., Fenter, P., Sturchio, N. C., Zhong, Z., & Bedzyk, M. J. (1999). X-ray standing wave  
592 study of arsenite incorporation at the calcite surface. *Geochimica et Cosmochimica*  
593 *Acta*, 63(19-20), 3153-3157. doi: https://doi.org/10.1016/S0016-7037(99)00242-2.

594 Comans, R. N., & Middelburg, J. J. (1987). Sorption of trace metals on calcite: Applicability of  
595 the surface precipitation model. *Geochimica et Cosmochimica Acta*, 51(9), 2587-2591.

596 Costigan, R. C., S. Dobson. (2001). Vanadium Pentoxide and other Inorganic Vanadium  
597 Compounds. Concise International Chemical Assessment Document 29. *Geneva: World*  
598 *Health Organization, World Health Organization*, 1-53.

599 Currell, M., Cartwright, I., Raveggi, M., & Han, D. (2011). Controls on elevated fluoride and  
600 arsenic concentrations in groundwater from the Yuncheng Basin, China. *Applied*  
601 *Geochemistry*, 26(4), 540-552. https://doi.org/10.1016/j.apgeochem.2011.01.012

602 Dietrich, S., Bea, S. A., Weinzettel, P., Torres, E., & Ayora, C. (2016). Occurrence and  
603 distribution of arsenic in the sediments of a carbonate-rich unsaturated zone.  
604 *Environmental Earth Sciences*, 75(2), 90. doi: https://doi.org/10.1007/s12665-015-  
605 4892-7

606 Elzinga, E., & Reeder, R. (2002). X-ray absorption spectroscopy study of Cu<sup>2+</sup> and Zn<sup>2+</sup>  
607 adsorption complexes at the calcite surface: Implications for site-specific metal  
608 incorporation preferences during calcite crystal growth. *Geochimica et Cosmochimica*  
609 *Acta*, 66(22), 3943-3954. doi: https://doi.org/10.1016/S0016-7037(02)00971-7

610 Elzinga, E., Reeder, R., Withers, S., Peale, R. E., Mason, R., Beck, K. M., & Hess, W. P. (2002).  
611 EXAFS study of rare-earth element coordination in calcite. *Geochimica et*  
612 *Cosmochimica Acta*, 66(16), 2875-2885.

- 613 Erban, L. E., Gorelick, S. M., Zebker, H. A., & Fendorf, S. (2013). Release of arsenic to deep  
614 groundwater in the Mekong Delta, Vietnam, linked to pumping-induced land  
615 subsidence. *Proceedings of the National Academy of Sciences*, *110*(34), 13751-13756.  
616 doi: <https://doi.org/10.1073/pnas.1300503110>
- 617 Fariás, S. S., Casa, V. A., Vázquez, C., Ferpozzi, L., Pucci, G. N., & Cohen, I. M. (2003). Natural  
618 contamination with arsenic and other trace elements in ground waters of Argentine  
619 Pampean Plain. *Science of the total Environment*, *309*(1), 187-199. doi:  
620 [https://doi.org/10.1016/S0048-9697\(03\)00056-1](https://doi.org/10.1016/S0048-9697(03)00056-1)
- 621 Farooqi, A., Masuda, H., & Firdous, N. (2007). Toxic fluoride and arsenic contaminated  
622 groundwater in the Lahore and Kasur districts, Punjab, Pakistan and possible  
623 contaminant sources. *Environmental Pollution*, *145*(3), 839-849.  
624 <https://doi.org/10.1016/j.envpol.2006.05.007>
- 625 Fendorf, S., Michael, H. A., & van Geen, A. (2010). Spatial and temporal variations of  
626 groundwater arsenic in South and Southeast Asia. *Science*, *328*(5982), 1123-1127. doi:  
627 DOI: 10.1126/science.1172974
- 628 Fiorentino, C. E., Paoloni, J. D., Sequeira, M. E., & Arosteguy, P. (2007). The presence of  
629 vanadium in groundwater of southeastern extreme the pampean region Argentina:  
630 Relationship with other chemical elements. *Journal of contaminant hydrology*, *93*(1-4),  
631 122-129. doi: <https://doi.org/10.1016/j.jconhyd.2007.02.001>
- 632 Frenguelli, J., & Teruggi, M. E. (1955). *Loess y limos pampeanos*: Olivieri y Dominguez.
- 633 García, M., Borgnino, L., Bia, G., & Depetris, P. (2014). Mechanisms of arsenic and fluoride  
634 release from Chacopampean sediments (Argentina). *International Journal of*  
635 *Environment and Health*, *7*(1), 41-57.
- 636 García, M. G., Lecomte, K. L., Stupar, Y., Formica, S., Barrionuevo, M., Vesco, M., Gallará, R., &  
637 Ponce, R. (2012). Geochemistry and health aspects of F-rich mountainous streams and  
638 groundwaters from sierras Pampeanas de Cordoba, Argentina. *Environmental Earth*  
639 *Sciences*, *65*(2), 535-545. doi: <https://doi.org/10.1007/s12665-011-1006-z>
- 640 Garrels RM, Christ CL (1965) Solutions, minerals, and equilibrium. Harper & Row. Harper's  
641 geoscience series, New York
- 642 Gérard, F., Clement, A., & Fritz, B. (1998). Numerical validation of a Eulerian hydrochemical  
643 code using a 1D multisolute mass transport system involving heterogeneous kinetically  
644 controlled reactions. *Journal of contaminant hydrology*, *30*(3-4), 201-216. doi:  
645 [https://doi.org/10.1016/S0169-7722\(97\)00047-8](https://doi.org/10.1016/S0169-7722(97)00047-8)
- 646 Glok Galli, M. G., Martínez, D. E., Kruse, E. E., Grondona, S. I., & Lima, M. L. (2014).  
647 Hydrochemical and isotopic characterization of the hydrological budget of a MAB  
648 Reserve: Mar Chiquita lagoon, province of Buenos Aires, Argentina. *Environmental*  
649 *earth sciences*, *72*(8), 2821-2835. <https://doi.org/10.1007/s12665-014-3187-8>
- 650 Gomez, M., Blarasin, M., & Martínez, D. (2009). Arsenic and fluoride in a loess aquifer in the  
651 central area of Argentina. *Environmental Geology*, *57*(1), 143-155. doi:  
652 <https://doi.org/10.1007/s00254-008-1290-4>
- 653 Guo, H., Liu, Z., Ding, S., Hao, C., Xiu, W., & Hou, W. (2015). Arsenate reduction and  
654 mobilization in the presence of indigenous aerobic bacteria obtained from high arsenic  
655 aquifers of the Hetao basin, Inner Mongolia. *Environmental pollution*, *203*, 50-59. doi:  
656 <https://doi.org/10.1016/j.envpol.2015.03.034>
- 657 Heredia, O. S., & Cirelli, A. F. (2009). Trace elements distribution in soil, pore water and  
658 groundwater in Buenos Aires, Argentina. *Geoderma*, *149*(3-4), 409-414. doi:  
659 <https://doi.org/10.1016/j.geoderma.2008.12.020>
- 660 Hopenhayn-Rich, C., Biggs, M. L., Fuchs, A., Bergoglio, R., Tello, E. E., Nicolli, H., & Smith, A. H.  
661 (1996). Bladder cancer mortality associated with arsenic in drinking water in Argentina.  
662 *Epidemiology*, 117-124.
- 663 Jang, Y. C., Somanna, Y., & Kim, H. (2016). Source, distribution, toxicity and remediation of  
664 arsenic in the environment—a review. *Int. J. Appl. Environ. Sci*, *11*(2), 559-581.

- 665 Joseph, T., Dubey, B., & McBean, E. A. (2015). Human health risk assessment from arsenic  
666 exposures in Bangladesh. *Science of the total Environment*, 527, 552-560. doi:  
667 <https://doi.org/10.1016/j.scitotenv.2015.05.053>
- 668 Kruse, E., & Ainchil, J. (2003). Fluoride variations in groundwater of an area in Buenos Aires  
669 Province, Argentina. *Environmental Geology*, 44(1), 86-89. doi:  
670 <https://doi.org/10.1007/s00254-002-0702-0>
- 671 Kumar, M., Das, N., Goswami, R., Sarma, K. P., Bhattacharya, P., & Ramanathan, A. (2016).  
672 Coupling fractionation and batch desorption to understand arsenic and fluoride co-  
673 contamination in the aquifer system. *Chemosphere*, 164, 657-667. doi:  
674 <https://doi.org/10.1016/j.chemosphere.2016.08.075>
- 675 Levy, D. B., Schramke, J. A., Esposito, K. J., Erickson, T. A., & Moore, J. C. (1999). The shallow  
676 ground water chemistry of arsenic, fluorine, and major elements: Eastern Owens Lake,  
677 California. *Applied Geochemistry*, 14(1), 53-65. [https://doi.org/10.1016/S0883-](https://doi.org/10.1016/S0883-2927(98)00038-9)  
678 [2927\(98\)00038-9](https://doi.org/10.1016/S0883-2927(98)00038-9)
- 679 Logan, W. S., & Rudolph, D. L. (1997). Microdepression-focused recharge in a coastal wetland,  
680 La Plata, Argentina. *Journal of Hydrology*, 194(1), 221-238. doi:  
681 [https://doi.org/10.1016/S0022-1694\(96\)03205-2](https://doi.org/10.1016/S0022-1694(96)03205-2)
- 682 Londoño, O. Q., Martínez, D. E., Dapeña, C., & Massone, H. (2008). Hydrogeochemistry and  
683 isotope analyses used to determine groundwater recharge and flow in low-gradient  
684 catchments of the province of Buenos Aires, Argentina. *Hydrogeology Journal*, 16(6),  
685 1113-1127. <https://doi.org/10.1007/s10040-008-0289-y>
- 686 Mahlknecht, J., Steinich, B., & De León, I. N. (2004). Groundwater chemistry and mass transfers  
687 in the Independence aquifer, central Mexico, by using multivariate statistics and mass-  
688 balance models. *Environmental Geology*, 45(6), 781-795.  
689 <https://doi.org/10.1007/s00254-003-0938-3>
- 690 Martínez, D., & Bocanegra, E. (2002). Hydrogeochemistry and cation-exchange processes in  
691 the coastal aquifer of Mar Del Plata, Argentina. *Hydrogeology Journal*, 10(3), 393-408.  
692 doi: <https://doi.org/10.1007/s10040-002-0195-7>
- 693 Martínez, D., Londoño, O. Q., Massone, H., Buitrago, P. P., & Lima, L. (2012).  
694 Hydrogeochemistry of fluoride in the Quequen river basin: natural pollutants  
695 distribution in the argentine pampa. *Environmental Earth Sciences*, 65(2), 411-420. doi:  
696 <https://doi.org/10.1007/s12665-011-0988-x>
- 697 Nicolli, H., Bundschuh, J., Blanco, M., Tujchneider, O., Panarello, H., Dapeña, C., & Rusansky, J.  
698 (2012a). Arsenic and associated trace-elements in groundwater from the Chaco-  
699 Pampean plain, Argentina: results from 100 years of research. *Science of the total*  
700 *Environment*, 429, 36-56. doi: <https://doi.org/10.1016/j.scitotenv.2012.04.048>
- 701 Nicolli, H., García, J., Falcón, C., & Smedley, P. (2012b). Mobilization of arsenic and other trace  
702 elements of health concern in groundwater from the Salí River Basin, Tucumán  
703 Province, Argentina. *Environmental geochemistry and health*, 34(2), 251-262. doi:  
704 <https://doi.org/10.1007/s10653-011-9429-8>
- 705 Nicolli, H., Suriano, J., Gomez Peral, M., Ferpozzi, L., & Baleani, O. (1989). Groundwater  
706 contamination with arsenic and other trace elements in an area of the Pampa,  
707 Province of Córdoba, Argentina. *Environmental Geology and Water Sciences*, 14(1), 3-  
708 16. doi: <https://doi.org/10.1007/BF01740581>
- 709 Nicolli, H. B., Bundschuh, J., García, J. W., Falcón, C. M., & Jean, J.-S. (2010). Sources and  
710 controls for the mobility of arsenic in oxidizing groundwaters from loess-type  
711 sediments in arid/semi-arid dry climates—Evidence from the Chaco—Pampean plain  
712 (Argentina). *Water research*, 44(19), 5589-5604. doi:  
713 <https://doi.org/10.1016/j.watres.2010.09.029>
- 714 Padhi, S., & Tokunaga, T. (2015). Surface complexation modeling of fluoride sorption onto  
715 calcite. *Journal of environmental chemical engineering*, 3(3), 1892-1900. doi:  
716 <https://doi.org/10.1016/j.jece.2015.06.027>

717 Palandri, J. L., & Kharaka, Y. K. (2004). A compilation of rate parameters of water-mineral  
718 interaction kinetics for application to geochemical modeling: GEOLOGICAL SURVEY  
719 MENLO PARK CA.

720 Paquette, J., & Reeder, R. J. (1995). Relationship between surface structure, growth  
721 mechanism, and trace element incorporation in calcite. *Geochimica et Cosmochimica*  
722 *Acta*, 59(4), 735-749. doi: [https://doi.org/10.1016/0016-7037\(95\)00004-J](https://doi.org/10.1016/0016-7037(95)00004-J)

723 Pokrovsky, O., & Schott, J. (2002). Surface chemistry and dissolution kinetics of divalent metal  
724 carbonates. *Environmental science & technology*, 36(3), 426-432. doi:  
725 10.1021/es010925u

726 Puntoriero, M. L., Cirelli, A. F., & Volpedo, A. V. (2015). Geochemical mechanisms controlling  
727 the chemical composition of groundwater and surface water in the southwest of the  
728 Pampean plain (Argentina). *Journal of Geochemical Exploration*, 150, 64-72. doi:  
729 <https://doi.org/10.1016/j.gexplo.2014.12.011>

730 Pye, K. (1995). The nature, origin and accumulation of loess. *Quaternary Science Reviews*,  
731 14(7), 653-667. doi: [https://doi.org/10.1016/0277-3791\(95\)00047-X](https://doi.org/10.1016/0277-3791(95)00047-X)

732 Reeder, R. J. (1996). Interaction of divalent cobalt, zinc, cadmium, and barium with the calcite  
733 surface during layer growth. *Geochimica et Cosmochimica Acta*, 60(9), 1543-1552. doi:  
734 [https://doi.org/10.1016/0016-7037\(96\)00034-8](https://doi.org/10.1016/0016-7037(96)00034-8)

735 Renard, F., Putnis, C. V., Montes-Hernandez, G., Ruiz-Agudo, E., Hovelmann, J., & Sarret, G.  
736 (2015). Interactions of arsenic with calcite surfaces revealed by in situ nanoscale  
737 imaging. *Geochimica et Cosmochimica Acta*, 159, 61-79. doi:  
738 <https://doi.org/10.1016/j.gca.2015.03.025>

739 Robertson, F. N. (1989). Arsenic in ground-water under oxidizing conditions, south-west United  
740 States. *Environmental geochemistry and Health*, 11(3-4), 171-185.  
741 <https://doi.org/10.1007/BF01758668>

742 Romero, F. M., Armienta, M. A., & Carrillo-Chavez, A. (2004). Arsenic sorption by carbonate-  
743 rich aquifer material, a control on arsenic mobility at Zimapán, Mexico. *Archives of*  
744 *environmental contamination and toxicology*, 47(1), 1-13.  
745 <https://doi.org/10.1007/s00244-004-3009-1>

746 Roman-Ross, G., Charlet, L., Cuello, G., & Tisserand, D. (2003). *Arsenic removal by gypsum and*  
747 *calcite in lacustrine environments*. Paper presented at the Journal de Physique IV  
748 (Proceedings).

749 Rouff, A. A., Elzinga, E. J., Reeder, R. J., & Fisher, N. S. (2004). X-ray Absorption Spectroscopic  
750 Evidence for the Formation of Pb (II) Inner-Sphere Adsorption Complexes and  
751 Precipitates at the Calcite– Water Interface. *Environmental science & technology*,  
752 38(6), 1700-1707. doi: 10.1021/es0345625

753 Sancha, A. M., & O’Ryan, R. (2008). Managing hazardous pollutants in Chile: arsenic *Reviews of*  
754 *Environmental Contamination and Toxicology Vol 196* (pp. 123-146): Springer.

755 Sayago, J., Collantes, M., Karlson, A., & Sanabria, J. (2001). Genesis and distribution of the Late  
756 Pleistocene and Holocene loess of Argentina: a regional approximation. *Quaternary*  
757 *International*, 76, 247-257. doi: [https://doi.org/10.1016/S1040-6182\(00\)00107-5](https://doi.org/10.1016/S1040-6182(00)00107-5)

758 Scanlon, B. R., Nicot, J., Reedy, R., Kurtzman, D., Mukherjee, A., & Nordstrom, D. K. (2009).  
759 Elevated naturally occurring arsenic in a semiarid oxidizing system, Southern High  
760 Plains aquifer, Texas, USA. *Applied Geochemistry*, 24(11), 2061-2071. doi:  
761 <https://doi.org/10.1016/j.apgeochem.2009.08.004>

762 Schulz, C., & Castro, E. (2003). *Estudio, planificación y explotación del agua subterránea: una*  
763 *trilogía utópica en la República Argentina [Study, planning and exploitation of*  
764 *groundwater: a utopian trilogy in the Argentina Republic]*. Paper presented at the  
765 Proceedings of III Congreso Argentino de Hidrogeología, Rosario, Argentina, Edit.  
766 Universidad Nacional de Rosario.

767 Smedley, P., Macdonald, D., Nicolli, H., Barros, A., Tullio, J., & Pearce, J. (2000). Arsenic and  
768 other quality problems in groundwater from northern La Pampa Province, Argentina.

- 769 Smedley, P. L., & Kinniburgh, D. G. (2001). Source and behavior of arsenic in natural waters.  
770 *United Nations synthesis report on arsenic in drinking water. World Health*  
771 *Organization, Geneva, Switzerland. [http://www.who.](http://www.who.int/water_sanitation_health/dwq/arsenicun1.pdf)*  
772 *int/water\_sanitation\_health/dwq/arsenicun1.pdf*, 1-61.
- 773 Smedley, P., Nicolli, H., Macdonald, D., Barros, A., & Tullio, J. (2002). Hydrogeochemistry of  
774 arsenic and other inorganic constituents in groundwaters from La Pampa, Argentina.  
775 *Applied Geochemistry*, 17(3), 259-284. doi: [https://doi.org/10.1016/S0883-](https://doi.org/10.1016/S0883-2927(01)00082-8)  
776 [2927\(01\)00082-8](https://doi.org/10.1016/S0883-2927(01)00082-8)
- 777 Smedley, P. L., Kinniburgh, D. G., Macdonald, D. M. J., Nicolli, H. B., Barros, A. J., Tullio, J. O., ...  
778 & Alonso, M. S. (2005). Arsenic associations in sediments from the loess aquifer of La  
779 Pampa, Argentina. *Applied geochemistry*, 20(5), 989-1016.
- 780 Smedley, P., Nicolli, H., Macdonald, D., & Kinniburgh, D. (2008). Arsenic in groundwater and  
781 sediments from La Pampa province, Argentina. *Bundschuh J.; Armienta MA; Birkle P.;*  
782 *Bhattacharya P*, 35-45.
- 783 Sjø, H. U., Postma, D., Jakobsen, R., & Larsen, F. (2008). Sorption and desorption of arsenate  
784 and arsenite on calcite. *Geochimica et Cosmochimica Acta*, 72(24), 5871-5884. doi:  
785 <https://doi.org/10.1016/j.gca.2008.09.023>
- 786 Sota de la, M., Puche, R., Rigalli, A., Fernandez, L., Benassatti, S., & Boland, R. (1997).  
787 Modificaciones en la masa o sea en la homeostasis de la glucosa en residentes de la zona  
788 de Bahía Blanca con alta ingesta espontánea de Fluor. *MEDICINA*, 57:417-420.
- 789 Steinhäuser, G., & Bichler, M. (2008). Adsorption of ions onto high silica volcanic glass. *Applied*  
790 *Radiation and Isotopes*, 66(1), 1-8. doi: <https://doi.org/10.1016/j.apradiso.2007.07.010>
- 791 Stipp, S., Lakshmanan, L., Jensen, J., & Baker, J. (2003). Eu<sup>3+</sup> uptake by calcite: Preliminary  
792 results from coprecipitation experiments and observations with surface-sensitive  
793 techniques. *Journal of contaminant hydrology*, 61(1-4), 33-43. doi:  
794 [https://doi.org/10.1016/S0169-7722\(02\)00111-0](https://doi.org/10.1016/S0169-7722(02)00111-0)
- 795 Stipp, S. L., Hochella Jr, M. F., Parks, G. A., & Leckie, J. O. (1992). CT<sup>2+</sup> uptake by calcite, solid-  
796 state diffusion, and the formation of solid-solution: Interface processes observed with  
797 near-surface sensitive techniques (XPS, LEED, and AES). *Geochimica et Cosmochimica*  
798 *Acta*, 56(5), 1941-1954. doi: [https://doi.org/10.1016/0016-7037\(92\)90321-9](https://doi.org/10.1016/0016-7037(92)90321-9)
- 799 Tesoriero, A. J., & Pankow, J. F. (1996). Solid solution partitioning of Sr<sup>2+</sup>, Ba<sup>2+</sup>, and CT<sup>2+</sup> to  
800 calcite. *Geochimica et Cosmochimica Acta*, 60(6), 1053-1063. doi:  
801 [https://doi.org/10.1016/0016-7037\(95\)00449-1](https://doi.org/10.1016/0016-7037(95)00449-1)
- 802 Tricart, J. (1973). Geomorfología de la Pampa Depresada: base para los estudios edafológicos y  
803 agronómicos: Secretaría de Estado de Agricultura y Ganadería de la Nación, Instituto  
804 Nacional de Tecnología Agropecuaria.
- 805 Turner, B. D., Binning, P., & Stipp, S. (2005). Fluoride removal by calcite: evidence for fluorite  
806 precipitation and surface adsorption. *Environmental science & technology*, 39(24),  
807 9561-9568. doi: 10.1021/es0505090
- 808 Vital, M., Martínez, D. E., Borrelli, N., & Quiroga, S. (2016). Kinetics of dissolution processes in  
809 loess-like sediments and carbonate concretions in the southeast of the province of  
810 Buenos Aires, Argentina. *Environmental Earth Sciences*, 75(17), 1231 .  
811 <https://doi.org/10.1007/s12665-016-6011-9>
- 812 Vital, M., Daval, D., Clément, A., Quiroga, S., Fritz, B., & Martínez, D. E. (2018). Importance of  
813 accessory minerals for the control of water chemistry of the Pampean aquifer,  
814 province of Buenos Aires, Argentina. *CATENA*, 160, 112-123. doi:  
815 <https://doi.org/10.1016/j.catena.2017.09.005>
- 816 Wang, Z., Guo, H., Xiu, W., Wang, J., & Shen, M. (2018). High arsenic groundwater in the Guide  
817 basin, northwestern China: Distribution and genesis mechanisms. *Science of the total*  
818 *Environment*, 640, 194-206. doi: <https://doi.org/10.1016/j.scitotenv.2018.05.255>
- 819 Wurl, J., Mendez-Rodríguez, L., & Acosta-Vargas, B. (2014). Arsenic content in groundwater  
820 from the southern part of the San Antonio-El Triunfo mining district, Baja California

821 Sur, Mexico. *Journal of Hydrology*, 518, 447-459. doi:  
822 <https://doi.org/10.1016/j.jhydrol.2014.05.009>  
823 Wyatt, C. J., Quiroga, V. L., Acosta, R. T. O., & Méndez, R. O. (1998). Excretion of arsenic (As) in  
824 urine of children, 7–11 years, exposed to elevated levels of As in the city water supply  
825 in Hermosillo, Sonora, Mexico. *Environmental research*, 78(1), 19-24.  
826 <https://doi.org/10.1006/enrs.1998.3844>  
827 Yang, K., Lu, H., Yue, S., Zhang, G., Lei, Y., La, Z., & Wang, W. (2018). Quantifying recent  
828 precipitation change and predicting lake expansion in the Inner Tibetan Plateau.  
829 *Climatic Change*, 147(1-2), 149-163. doi: <https://doi.org/10.1007/s10584-017-2127-5>  
830 Zabala, M., Manzano, M., & Vives, L. (2015). The origin of groundwater composition in the  
831 Pampeano Aquifer underlying the Del Azul Creek basin, Argentina. *Science of the total*  
832 *Environment*, 518, 168-188. doi: <https://doi.org/10.1016/j.scitotenv.2015.02.065>  
833 Zachara, J., Cowan, C., & Resch, C. (1991). Sorption of divalent metals on calcite. *Geochimica et*  
834 *Cosmochimica Acta*, 55(6), 1549-1562. doi: [https://doi.org/10.1016/0016-](https://doi.org/10.1016/0016-7037(91)90127-Q)  
835 [7037\(91\)90127-Q](https://doi.org/10.1016/0016-7037(91)90127-Q)  
836 Zárata, M. A. (2003). Loess of southern South America. *Quaternary Science Reviews*, 22(18),  
837 1987-2006. doi: [https://doi.org/10.1016/S0277-3791\(03\)00165-3](https://doi.org/10.1016/S0277-3791(03)00165-3)  
838  
839  
840



**Table 1. Highest concentrations of major elements in the first test (T1) and second test (T2) of the flow-through and final concentration of the first test (TF1) conducted with the samples of loess and calcrete collected in the area of Mar del Plata.**

	LOESS			CALCRETE		
	T1	TF1	T2	T1	TF1	T2
Ca <sup>2+</sup>	4.8	0.06	0.16	0.64	0,2	0,37
Na <sup>+</sup>	3.3	0.2	0.09	3.2	0,5	0,58
SiO <sub>2</sub>	0.24	0.04	0.21	0,29	0,20	0,16
SO <sub>4</sub> <sup>-2</sup>	0.7	0.02	0.01	0,40	n/d	0,05
K <sup>+</sup>	0.14	0.05	0.015	0.1	0.03	0.08
Cl <sup>-</sup>	21	0.01	0.1	7,99	0,1	0,1

\* mmol.l<sup>-1</sup>

**Table 2. Arsenic content of solutions in contact with calcrete in flow-through experiments with tests T1 and T2 from 3 locations of the Buenos Aires Province.**

	T1				T2			
	t1	t5	t30	t60	t1	t5	t30	t60
Otamendi	det <0.005	det <0.005	no det <0.002	no det <0.002	det <0.005	det <0.005	det <0.005	det <0.005
Tandil	det <0.005	det <0.005	det <0.005	no det <0.002	det <0.005	det <0.005	no det <0.002	no det <0.002
Tres arroyos	det <0.005	det <0.005	det <0.005	no det <0.002	det <0.005	det <0.005	no det <0.002	no det <0.002

T1: Test 1 - T2: Test 2

t: time in minutes

Det: detected - No det: not detected

\*  $\mu\text{mol.l}^{-1}$

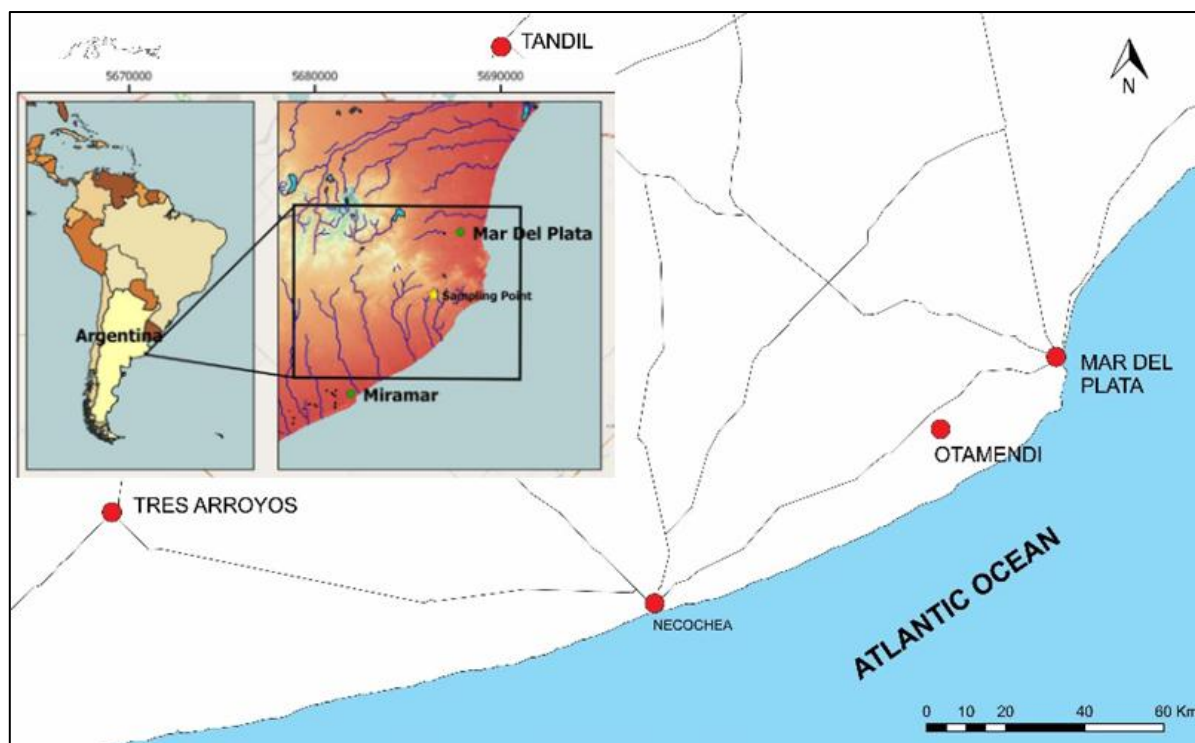


Figure 1. Location of the sampling points (indicate by red dots on the map)

## Figure2

[Click here to download Figure: figure2.docx](#)

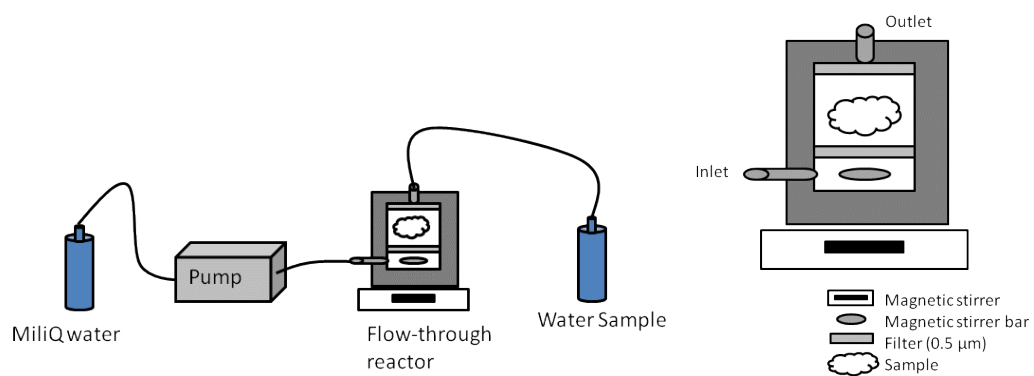


Figure 2. Schematic diagrams of the flow-through experiment and reactor. The deionized water (pH 5.7) is continuously pumped through the reactor at a flow rate of  $5 \text{ ml} \cdot \text{min}^{-1}$  where the loess or calcrite samples were previously introduced.

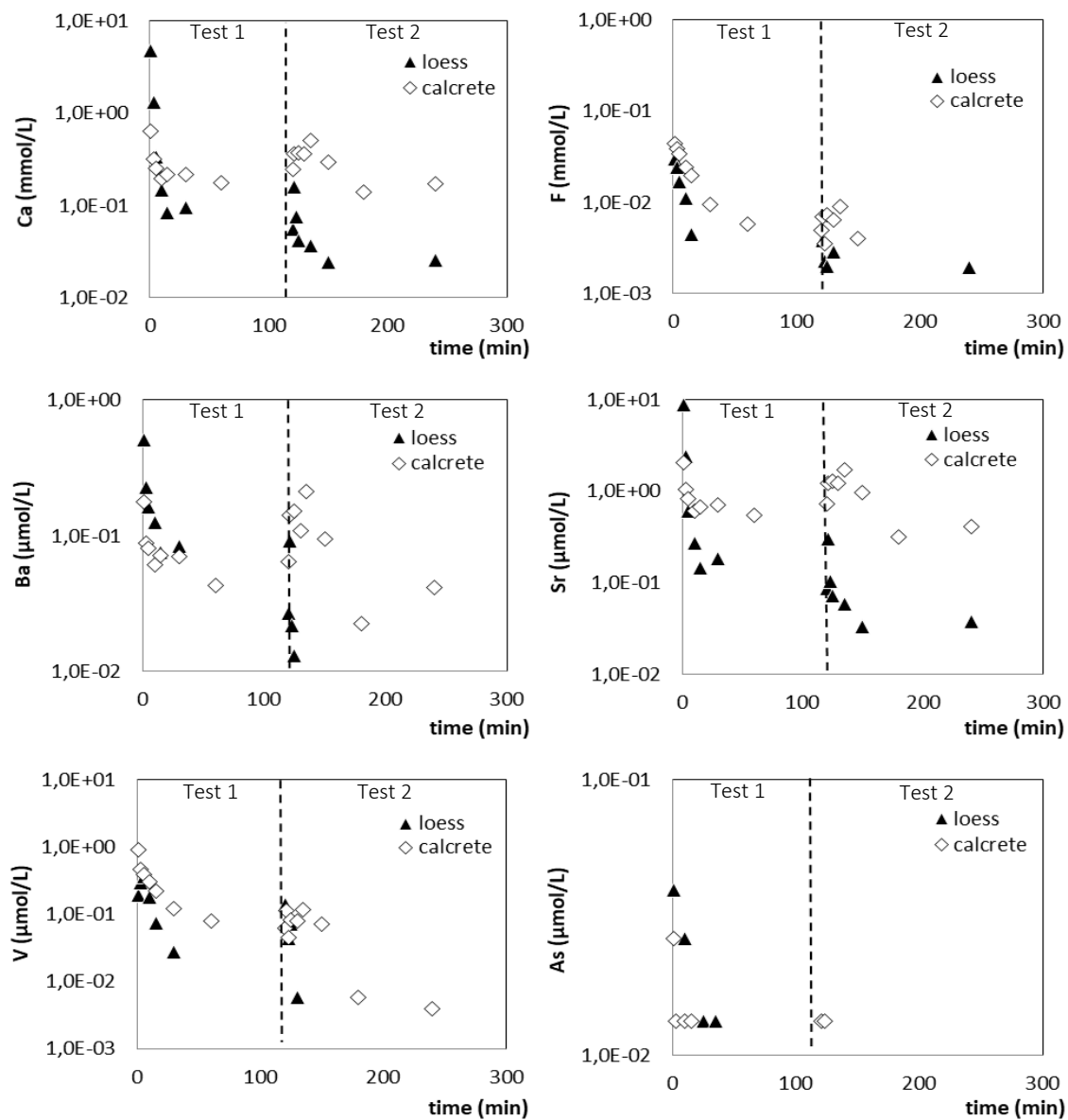


Figure 3. Release of trace elements in the flow-through experiment test 1 (T1) and test 2 (T2) conducted with the loess and calcrete samples from the area of Mar del Plata.

# Figure4

[Click here to download Figure: figure4.docx](#)

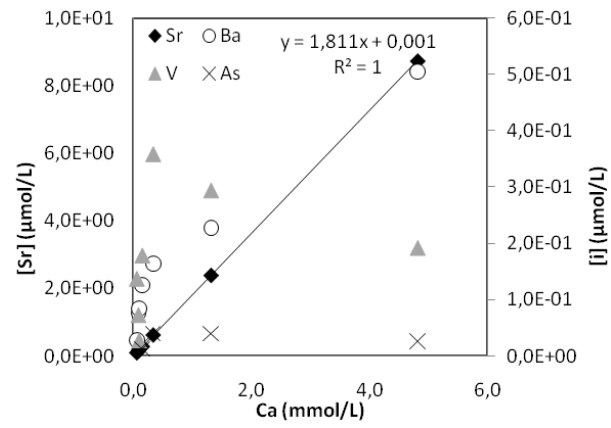


Figure 4. Correlation between Ca and trace elements (Ba, Sr, V, As) in the flow-through experiment test T1 conducted with loess.

# Figure5

[Click here to download Figure: figure5.docx](#)

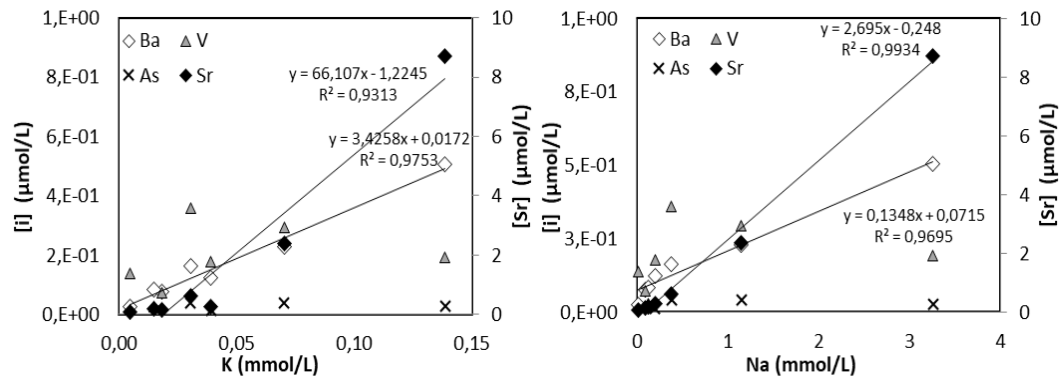


Figure 5. Correlation between  $\text{Na}^+$ ,  $\text{K}^+$  and trace elements ( $\text{Ba}^{2+}$ ,  $\text{Sr}^{2+}$ ) in the flow through experiment

Test T1 conducted with loess.

# Figure6

[Click here to download Figure: figure6.docx](#)

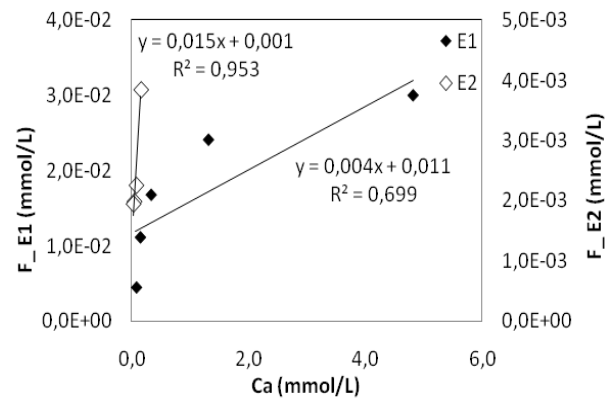


Figure 6. Correlation between  $\text{Ca}^{2+}$  and  $\text{F}^-$  release in T1 and T2 flow-through experiments conducted with loess.



**Figure7**

[Click here to download Figure: figure7.docx](#)

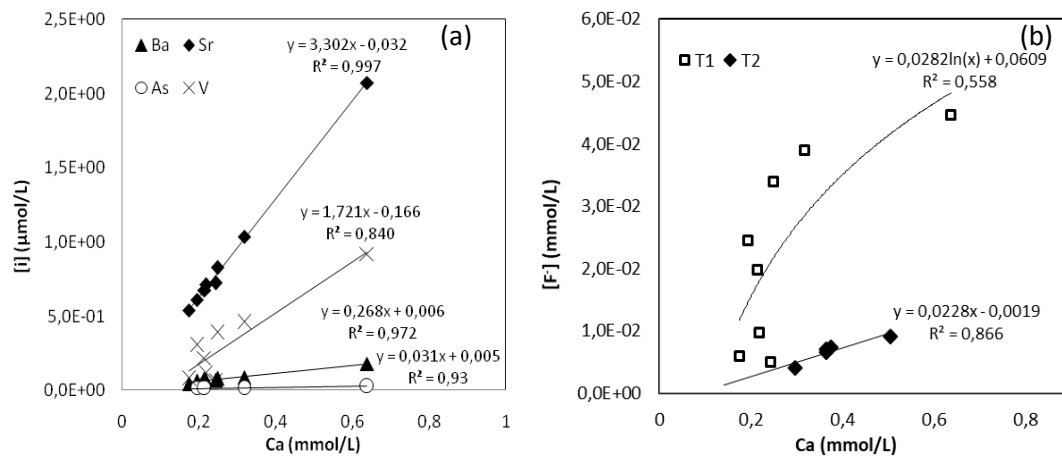


Figure7. Correlations between Ca<sup>2+</sup> and Ba<sup>2+</sup>, Sr<sup>2+</sup>, As, V in the flow through experiments T1 (a) and between Ca<sup>2+</sup> and F<sup>-</sup> (b) in the test T1 and T2 conducted on calcrete samples.

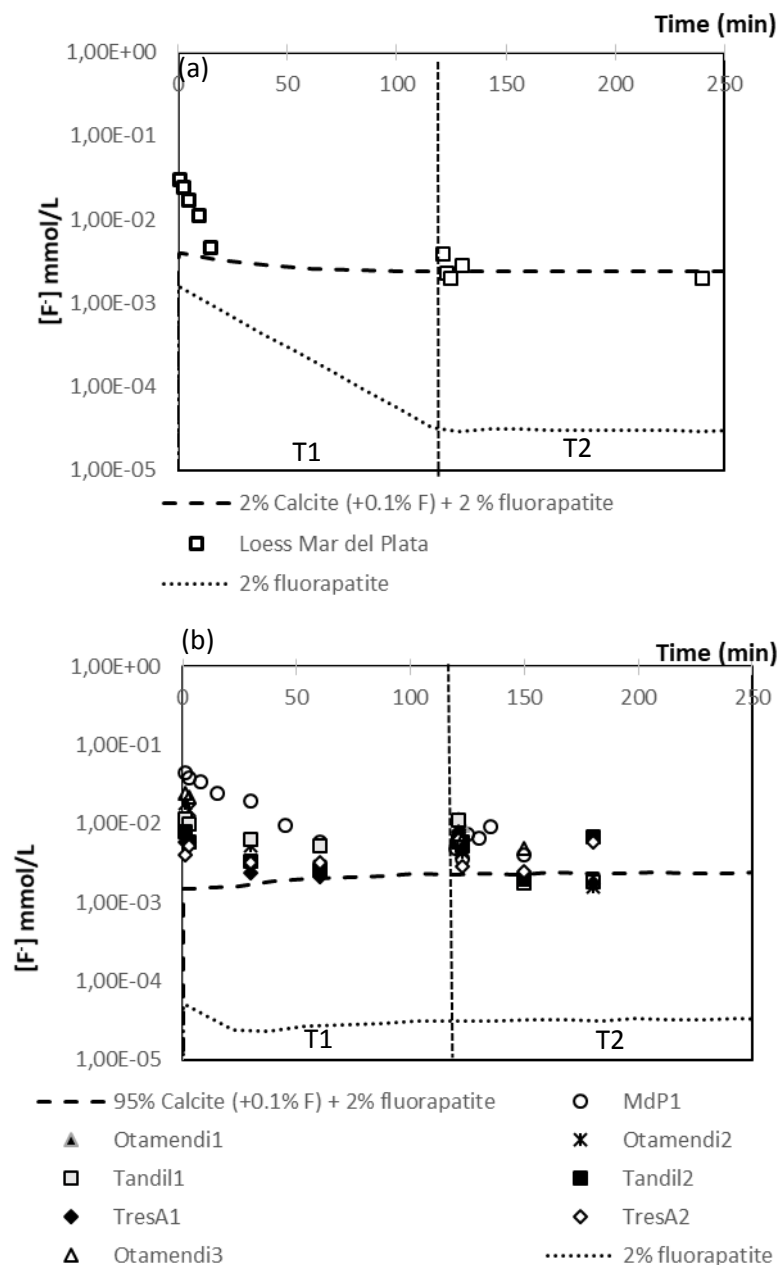


Figure 8. Simulations of fluoride release for loess (a) and calcrete (b) experiments including accessory minerals. The kirmat simulation for loess and calcrete were first realized with 2% of fluorapatite. Then, another kirmat simulation for loess was realized with 2% Calcite containing 0.1% impurity of fluoride and 2% of fluorapatite. Another kirmat simulation for calcrete was realized with 95% Calcite containing 0.1% impurity of fluoride and 2% of fluorapatite. The Kirmat simulations were compared to the flow-through experiments T1 and T2 on the loess sample from Mar del Plata (MdP) and the calcrete samples from Mar del Plata (MdP), Otamendi, Tandil and Tres Arroyos (TresA), in the province of Buenos Aires.